NITROGEN AND SULFUR-DOPED CARBON QUANTUM DOTS USED AS FLUORESCENT PROBES

H. Li [1], Y. Zhang [1], X. Pang [1], X. Niu [1], D. Zhang [1], H. Feng [1], H. Fan [2], K. Wang [1*]

[1] College of Petrochemical Technology at Lanzhou University of Technology, Lanzhou, China; e-mail: wangkj80@163.com
[2] Nazarbayev University, Nur-Sultan, Kazakhstan

Using hydrolyzed olive leaves as a carbon source and thiourea as a dopant, nitrogen-sulfur co-doped carbon quantum dots (NS-CQDs) were synthesized in the present work. The as-prepared NS-CQDs exhibited quasispherical morphology with an average particle size of 2–5 nm. Functional groups such as carboxyl and hydroxyl groups distributed on the surface of NS-CQDs were suggested to contribute to the good water solubility, biocompatibility, and strong fluorescence. Amphotericin B (AMB) was found to enhance the fluorescence intensity of NS-CQDs, whereas Fe(III) quenched the fluorescence of NS-CQDs. Taking advantage of such fluorescent characteristics, we established herein a quantitative method of measuring the content of AMB and Fe^{3+} in water, with detection limits of 10.0 and 7.4 μM, respectively.

Keywords: *carbon quantum dots, nitrogen and sulfur doping, detection, amphotericin B, fluorescence*.

ФЛУОРЕСЦЕНТНЫЙ ЗОНД НА ОСНОВЕ ЛЕГИРОВАННЫХ АЗОТОМ И СЕРОЙ УГЛЕРОДНЫХ КВАНТОВЫХ ТОЧЕК

H. Li [1], Y. Zhang [1], X. Pang [1], X. Niu [1], D. Zhang [1], H. Feng [1], H. Fan [2], K. Wang [1*]

УДК 535.37

[1] Колледж нефтехимических технологий Ланьчжоуского технологического университета, Ланьчжоу, Китай; e-mail: wangkj80@163.com
[2] Назарбаев Университет, Нур-Султан, Казахстан

(Поступила 13 сентября 2021)

С использованием гидролизованных листьев оливы в качестве источника углерода и тиомочевины в качестве легирующей примеси синтезированы углеродные квантовые точки, легированные азотом и серой (NS-CQDs). Продемонстрирована квазисферическая морфология полученных NS-CQDS со средним размером частиц 2—5 нм. Предположено, что функциональные группы (карбоксильные и гидроксильные), распределенные на поверхности NS-CQDs, способствуют хорошей растворимости в воде, биосовместимости и сильной флуоресценции. Обнаружено, что амфотерицин B (AMB) усиливает интенсивность флуоресценции NS-CQDs, в то время как Fe(III) подавляет их флуоресценцию. Разработан количественный метод измерения содержания AMB и Fe^{3+} в воде с пределами обнаружения 10.0 и 7.4 мкм.

Ключевые слова: *углеродные квантовые точки, легирование азотом и серой, обнаружение, амфотерицин B, флуоресценция.*

Introduction. Although the mechanism underlying the fluorescence emission of carbon quantum dots (CQDs) has not been fully elucidated, it has been hypothesized that the quantum defects formed on the surface because of the size (<10 nm) are mainly responsible for the fluorescence emission [1]. Since their discovery [2], CQDs have attracted widespread attention. In addition to their fluorescent properties, CQDs have many other advantages, such as excellent biocompatibility, low toxicity, low cost, a wide range of synthetic materials, and ease of synthesis [3–6]. It has been found that the fluorescent properties of CQDs may be adjusted through the modification of the surface functional groups [7]. Heteroatomic doping has been proven to

be an effective means of improving the optical performance of CQDs [8]. Additionally, CQDs have been extensively applied in the fields of catalysis [9, 10], bioimaging [11], medical diagnosis [12], and sensors [13, 14]. In particular, it has strong photoluminescence (PL), is easy to synthesize, and has excellent water solubility, biocompatibility, low toxicity, photobleaching resistance, and environmental protection [15–17].

If the fluorescence of the CQDs is caused by the surface quantum defect, the fluorescence intensity should be proportional to the total population of the surface quantum defects. However, owing to the surface functional groups, the particles of CQDs tend to aggregate through intermolecular interactions, and such aggregation reduces the population of quantum defects. Our previous work indicated that the fluorescence intensity of a CQDs aqueous solution could be enhanced by adding amoxicillin [18]. The enhancement of fluorescence was ascribed to the large aggregation reduction of CQDs particles caused by the adsorption of amoxicillin molecules on the surface of CQDs, which could be used as a passivation reagent. Owing to their fluorescent property, CQDs have been used as biosensors to detect certain cations, anions, organics, and antibiotics, such as Fe^{3+} [19–21], Cr^{5+} [22], Mo^{6+} [23], Co^{2+} [24], Hg^{2+} [25, 26], I^- [27], $ONOO^-$ [28], testosterone [29], hyaluronidase [30], selenite [31], glutathione [32], tetracycline [33], and amoxicillin [18].

Amphotericin B (AMB) is a polyene antifungal drug. It affects the permeability of the fungal cell membrane through complexation with the sterol, resulting in the death of cells because of the leakage of substances inside the fungal cell. AMB, as a broad-spectrum antifungal drug, is widely used to treat visceral or systemic infections caused by serious deep fungi. AMB itself is highly toxic, leading to severe permanent renal impairment [34]. The quantitative detection of AMB has been performed with biological matrices, mainly using HPLC coupled with UV or MS detectors [35–39]. With the widespread use of AMB in the clinic, the presence of AMB in the environment is likely to lead to the development of fungal drug resistance. Quantitative measurement becomes urgent to control the AMB level released into the environment. Thanks to our experience in the detection of other antibiotics using CQDs, we attempted herein to detect AMB in aqueous solution using the as-prepared NS-CQDs.

Experimental. Olive leaves were obtained in the olive planting area of Longnan city, Gansu Province, China. Amphotericin B was purchased from Shanghai Yuanye Biotechnology. Ferric chloride, thiourea, nitric acid, sulfuric acid, hydrochloric acid, anhydrous ethanol, sodium hydroxide, sodium chloride, and dichloromethane were purchased from China Pharmaceutical Holding Chemical Reagent. Sucrose, glucose, ascorbic acid, tryptophan, aspartic acid, L-cysteine, KBr, $Ca(NO_3)_2$, NaF, $BaCl_2$, $AlCl_3$, $CaCl_2$, KCl, $MgCl_2$, $MnCl_2$, NH_4Cl, $SrCl_2$, and $ZnCl_2$ were analytically pure (AR) reagents. All reagents were used directly without any further purification. Deionized water was prepared using a Milli-Q-Plus system (18.2 MΩ).

Transmission electron microscopy (TEM) analyses were carried out using a JEOL JEM2100 instrument operating at 200 kV. The samples for TEM analysis were prepared by dropping a droplet of the ethanol solution of the product onto carbon-coated copper grids and drying at room temperature. Fourier transform infrared spectroscopy (FTIR) spectra were measured on a Nicolet AVATAR 360 FT-IR spectrophotometer. X-ray diffraction (XRD) analysis was carried out using a Shimadzu XRD-6000 spectrometer. Photoluminescence (PL) and UV-Vis spectra of the as-prepared CQDs were taken at room temperature in water. The PL spectra were obtained using a LS-55 spectrophotometer (PerkinElmer, USA), and UV-Vis spectra were obtained using a UV-2102PC spectrophotometer (Unico, USA). All optical measurements were carried out at room temperature under ambient conditions.

Synthesis of NS-CQDs. Olive leaf powder was immersed completely in concentrated sulfuric acid for 12 h. Subsequently, 50 mL ultrapure water was added. Then, the mixture was transferred into a 100-mL Teflon-lined autoclave and heated at 120°C for 2 h in an oven. After cooling to room temperature, sodium hydroxide was added to the mixture until the pH reached 7. Then, 3 g of thiourea was added. The mixture was transferred into an autoclave again and heated at 180°C for 8 h. Thereafter, the larger solid particles were filtered by a 0.22-μm Millipore membrane, and then the obtained products were washed with dichloromethane to remove the organic impurities. The obtained samples were dispersed into ethanol and centrifuged at 12,000 r/min for 20 min. Following dialysis for 48 h in a 1000-Da dialysis bag, the obtained NS-CQDs mother solution was freeze-dried at −60°C to prepare the NS-CQDs powder.

AMB detection by using NS-CQDs. To demonstrate the sensing capability of the as-prepared NS-CQDs, a calibration curve was generated using PL spectroscopy within the concentration range of AMB from 0 to 100 μM; the stability of the fluorescence of NS-CQDs was tested under high ionic strength conditions; and the selectivity was identified by adding some common ions and small molecules. All PL intensities were measured using an excitation wavelength of 350 nm (CQDs, 5 μg/mL). All measurements were performed under the same conditions at room temperature and repeated at least three times.

Fe(III) detection by using NS-CQDs. Ten different cations were used for fluorescence detection, and Fe(III) within the concentration range 0–100 μM indicated the best quenching efficiency. All measurements were performed under the same conditions at room temperature and repeated at least three times.

Results and discussion. *Synthesis and characterization of NS-CQDs*. The TEM patterns depicted in Fig. 1a show that the as-prepared NS-CQDs are well dispersed particles with uniform sizes of 2–5 nm. The XRD spectrum in Fig. 1b exhibits broad diffraction peaks at 2θ of 22°, suggesting that the NS-CQDs consist of amorphous carbon. In Figure 1c, the FT-IR spectrum shows a broad absorption band centered at 3380 cm^{-1}, representing O-H stretching. Two bands located at 1607 and 1432 cm^{-1} can be assigned to the asymmetric and symmetric stretching vibrations of the carboxyl anions, respectively. Such assignment implies that the O-H group identified through the band at 3380 cm^{-1} is not necessarily part of the carboxyl group; rather, it is independently distributed on the surface of CQDs.

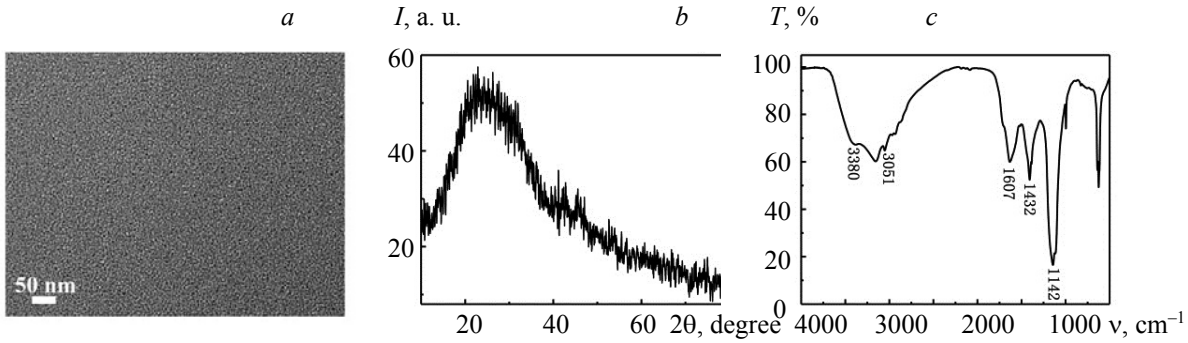

Fig. 1. TEM image (a), XRD pattern (b), and FTIR spectra (c) of the as-prepared NS-CQDs.

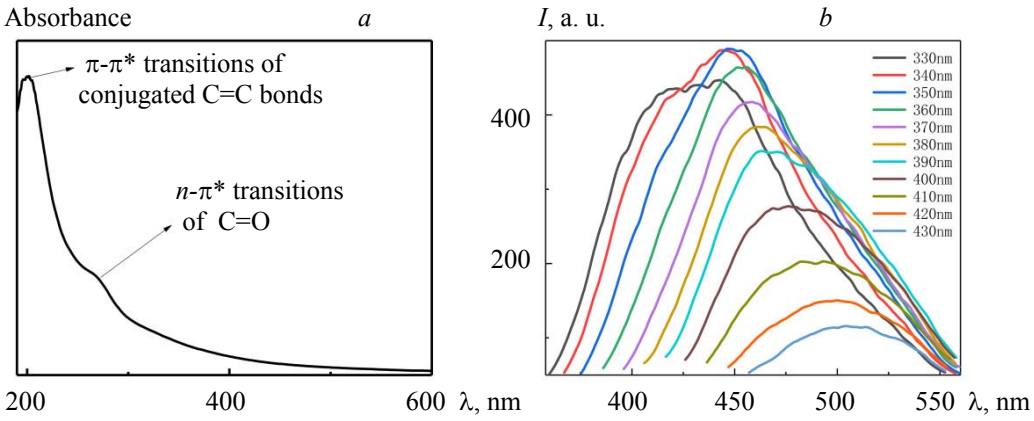

Fig. 2. (a) UV-Vis absorption spectrum of the as-prepared NS-CQDs, and (b) PL spectra of the as-prepared NS-CQDs under a series of excitation wavelengths.

The UV-Visible spectrum of the as-prepared NS-CQDs indicates two absorption bands at 200 and 263 nm. The band at 200 nm corresponds to the π-π^* transition of the C=C bond, whereas the band at 263 nm represents the n-π^* transition of the C=O bond (Fig. 2a).

The fluorescence of NS-CQDs centered at 450 nm exhibits the strongest intensity at the excitation wavelength of 350 nm (Fig. 2b). Overall, the fluorescence indicates an excitation wavelength dependence. As the excitation wavelength increases from 330 to 430 nm, the emission wavelength also increases, but the fluorescence intensity decreases significantly as the excitation wavelength is longer than 370 nm.

As mentioned earlier, many factors, such as pH and ionic strength, may intervene in the aggregation status of the particles of CQDs and lead to some change in the fluorescence properties. The pH dependence of the fluorescence of NS-CQDs was studied within the pH range from 1 to 14. Figure 3a shows the relatively lower fluorescence intensities at extremely low and high pH values, considering the possible strong inter-

action among the particles of CQDs under extremely acidic or basic conditions. Overall, the as-prepared NS-CQDs present good stability over a wide pH range, which makes them excellent fluorescence probes.

The ionic strength dependence of the fluorescence properties of NS-CQDs was tested in NaCl solutions with concentrations ranging from 0 to 1.0. According to Fig. 3b, the fluorescence intensity is largely independent of the ionic strength in the solution, which is particularly beneficial for measurements at high ionic strength. This finding ensures that NS-CQDs have great potential for sensing applications under more complex and physiological conditions.

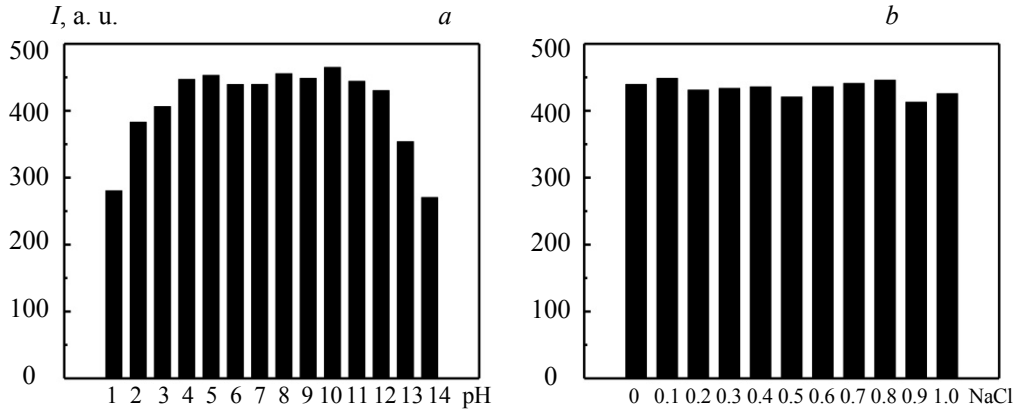

Fig. 3. (a) Effect of pH on the PL intensity of the as-prepared NS-CQDs; (b) PL intensity of as-prepared NS-CQDs in NaCl aqueous solution (pH 7) against ionic strength.

Detection of AMB. Taking advantage of the above, the prepared NS-CQDs are used as a fluorescence sensor for the sensitive and selective detection of AMB (Fig. 4a). A calibration curve was established between the fluorescence intensity and the concentration of AMB within the range 0 to 100 μM. Additionally, when the AMB concentration is within the range 0–100 μM, I/I_0 shows a linear relationship (Fig. 4b). The linear equation is $I/I_0 = 1.18575 + 0.01052$ [AMB] ($R^2 = 0.88545$, I and I_0 are the PL intensities in the presence and absence of AMB, respectively), which indicates that it is completely feasible to detect AMB with NS-CQDs. In the current work, the lower measurement limit of AMB was determined to be 9.2 μM (9.2 ng/mL).

As indicated in Fig. 4c, the fluorescence of NS-CQDs experiences an immediate increase upon the addition of AMB at the excitation wavelength of 350 nm. To evaluate the selectivity of the prepared NS-CQDs, some potential interfering compounds, including sucrose, glucose, ascorbic acid, tryptophan, aspartic acid, L-cysteine, KBr, $Ca(NO_3)_2$, and NaF (each 250 μM), were introduced to detect the impact on the fluorescence of NS-CQDs under the same conditions. The results in Fig. 4d show that the combination of these potential interfering compounds had little impact on the overall fluorescence. Thus, the prepared NS-CQDs selectively and quantitatively detect AMB levels in aqueous solution.

The possible mechanism of the fluorescence enhancement upon the addition of AMB is presented herein. As evidenced by the FT-IR spectrum, a significant amount of hydrophilic functional groups, such as carboxylic anions and hydroxyl groups, are distributed on the surface of NS-CQDs, which opens up great opportunities for intermolecular hydrogen bonding with the molecules of AMB. On the other hand, part of the surface of the AMB molecules is largely nonpolar and thus leads to repulsion among the AMB molecules. Hence, the AMB molecules attached to the surface of NS-CQDs through intermolecular hydrogen bonds act as a passivation reagent that effectively prevents the particles of CQDs from aggregating together. The attachment of AMB helps to enhance the population of surface defects of NS-CQDs, resulting in the enhancement of PL strength [40–42]. The exact mechanism of fluorescence enhancement requires further study.

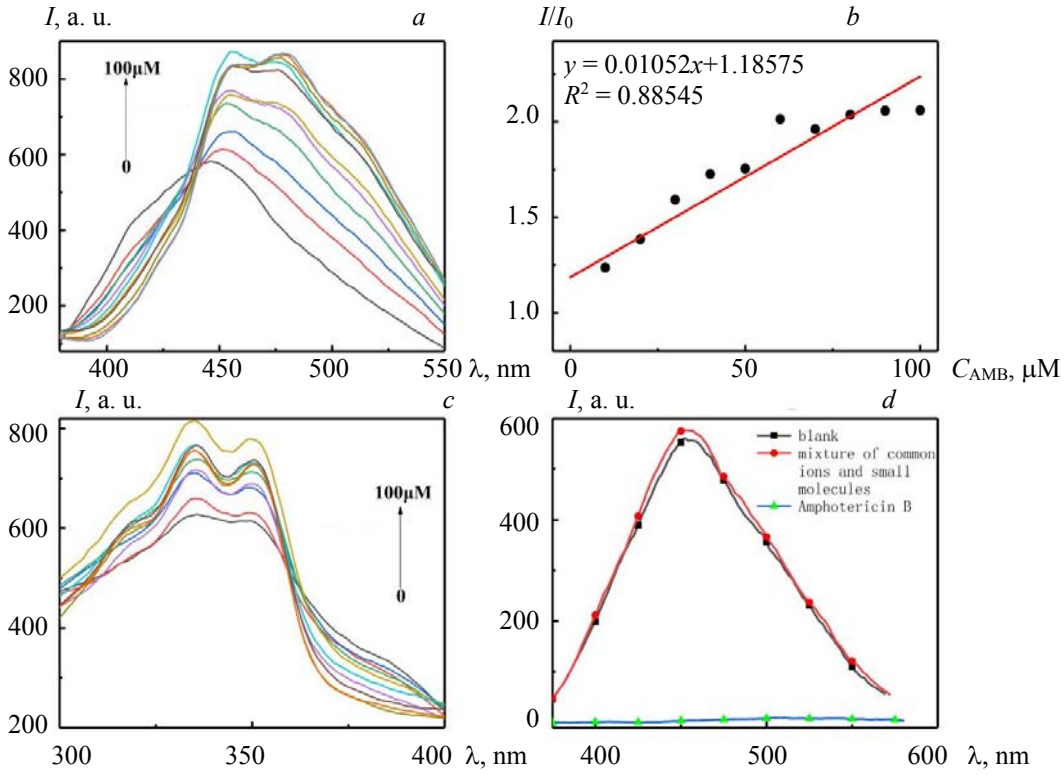

Fig. 4. (a) PL spectra of NS-CQDs dispersions in the presence of different concentrations of AMB from 0 to 400 μM, NS-CQDs, 5 μg/mL; (b) The linear plot of I/I_0 versus AMB concentration within the range 0 to 100 μM; (c) PL absorption spectra of NS-CQDs dispersion in the presence of different concentrations of AMB 0–400 μM; (d) The PL intensity of the as-prepared NS-CQDs (5 μg/mL) in the presence of various common ions and small molecules (250 μM for each). Data are presented as the average of three independent measurements ($N = 3$).

TABLE 1. Different AMB Detection Methods

Method	Detection range, μM	Detection limit, μg/mL	Sample
Spectrophotometric method	0.2–2.4	0.2	Serum, urine
HPLC	0.05–200	0.05	Human serum
LC/MS/MS	–	2	Plasma
This work	10.0–100.0	9.2 ng/mL	Water solution

Table 1 compares the fluorescent probe with other sensing platforms used for the detection of AMB. Compared with other methods, this work has a lower detection limit and wider linear range.

Detection of Fe(III). The fluorescence of NS-CQDs was quenched upon the addition of Fe(III), as indicated in Figs. 5a,b. A calibration curve was established within the concentration range 0 to 700 μM (Figs. 5c,d) with a great linear correlation, and the detection limit was identified as 7.4150 μM. Additionally, Al^{3+}, Ba^{2+}, Ca^{2+}, K^{+}, Mg^{2+}, Mn^{2+}, NH_4^{+}, Sr^{2+}, and Zn^{2+} did not exhibit significant interference.

The possible mechanism of fluorescence quenching is discussed here. It is likely that Fe(III) coordinates with the functional groups on the surface of CQDs, and charge transfer develops between CQDs and the formed metal complexes. Furthermore, the formed metal complexes between Fe(III) and the surface functional groups do not emit fluorescence at the excitation wavelength of 350 nm.

The opposite impact of Fe^{3+} and AMB on the fluorescence of CQDs in the present work makes it difficult to apply the present quantitative method to the simultaneous measurement of Fe^{3+} and AMB in water samples. The application of the present method demands some treatment of the sample to separate Fe^{3+} and AMB from each other.

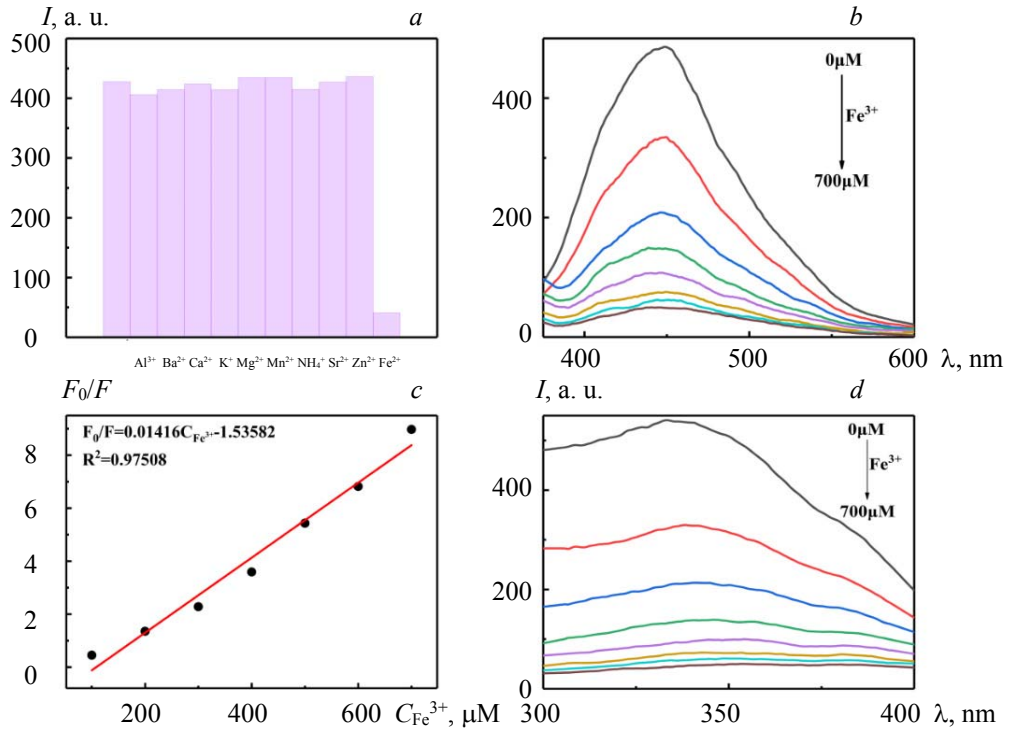

Fig. 5. (a) Fluorescence emission intensity of NS-CQDs in the presence of ten different cations; (b) PL spectra of NS-CQDs dispersion in the presence of different concentrations of Fe(III) from 0 to 700 μM; (c) The linear plot of I/I_0 versus Fe(III) concentration within the range 0 to 700 μM, PL absorption spectra of NS-CQDs dispersion in the presence of different concentrations of Fe(III) from 0 to 700 μM. NS-CQDs, 5 μg/mL; (d) PL absorption spectra of NS-CQDs dispersion in the presence of different concentrations of Fe(III) from 0 to 700 μM, NS-CQDs, 5 μg/mL.

Conclusions. The present work develops a facial synthesis of NS-CQDs using olive leaves and thiourea, which exhibited high water solubility and strong fluorescence emission at 450 nm, with excitation at 350 nm. Such strong fluorescence is largely independent of the pH and ionic strength in the aqueous solution. The addition of AMB to the aqueous solution of NS-CQDs enhances the fluorescence intensity, whereas the addition of Fe(III) quenches the fluorescence intensity. These effects were used to develop a quantitative detection of AMB and Fe(III) in aqueous solution, wherein both methods indicated a high selectivity. The detection limits of 10.0 and 7.4 μM were identified for AMB and Fe(III), respectively. The fluorescence enhancement with the NS-CQDs-AMB system was discussed, as well as the fluorescence quenching with the NS-CQDs-Fe(III) system. The molecules of AMS were believed to act as a passivation agent that stopped the particles of NS-CQDs from aggregating and resulted in an increase in the fluorescence intensity, whereas Fe(III) likely formed metal complexes with the surface functional group, leading to a charge transfer that was responsible for the fluorescence quenching. We thereafter developed a rapid-response, stable, highly sensitive, and selective detection method for the quantitative determination of trace amounts of AMB or Fe(III) in aqueous solution when they do not coexist in the sample. The present method of quantitative analysis of AMB is simple, sensitive, selective, and highly accurate, and may be applied to the direct determination of AMB levels in environmental samples or coupled with HPLC to achieve the measurement of trace amounts of AMB in biological metrics.

Acknowledgments. This work was supported by the National Natural Science Foundations of China (Grant Nos. 21867015 and 22065021), the Key Research Program of Gansu Province (21YF5GA076), the Province Natural Science Foundations of Gansu (Grant Nos. 20JR5RA453 and 21JR7RA213) and the Hongliu Outstanding Youth Teacher Cultivate Project of Lanzhou University of Technology.

REFERENCES

1. H. Li, R. Liu, S. Lian, Y. Liu, H. Huang, Z. Kang, *Nanoscale*, **5**, 3289 (2013).
2. X. Xu, R. Ray, Y. Gu, H. J. Ploehn, L. A. Gearheart, K. Raker, W. A. Scrivens, *J. Am. Chem. Soc*., **126**, 12736 (2004).
3. C. Wang, H. Lin, Z. Xu, Y. Huang, M. G. Humphrey, C. Zhang, *ACS Appl. Mater. Int*., **8**, 6621 (2016).
4. S. Qu, X. Wang, Q. Lu, X. Liu, L. Wang, *Angew. Chem. Int. Edit*., **51**, 12215 (2012).
5. E. A. Chandross, *Chem. Mater*., **26**, 6083 (2014).
6. C. Ding, A. Zhu, Y. Tian, *Acc. Chem. Res*., **47**, 20 (2014).
7. Y. Sun, B. Zhou, Y. Lin, W. Wang, K. A. S. Fernando, P. Pathak, M. J. Meziani, B. A. Harruff, X. Wang, H. Wang, *J. Am. Chem. Soc*., **128**, 7756 (2006).
8. L. Li, T. Dong, *J. Mater. Chem. C*, **6**, 7944 (2018).
9. F. Wang, P. Chen, Y. Feng, Z. Xie, Y. Liu, Y. Su, Q. Zhang, Y. Wang, K. Yao, W. Lv, *Appl. Catal. B*, **207**, 103 (2017).
10. G. A. M. Hutton, B. C. M. Martindale, E. Reisner, *Chem. Soc. Rev*., **46**, 6111 (2017).
11. J. Zhang, S. Yu, *Mater. Today*, **19**, 382 (2016).
12. J. Shangguan, J. Huang, D. He, X. He, K. Wang, R. Ye, X. Yang, T. Qing, J. Tang, *Anal. Chem*., **89**, 7477 (2017).
13. J. Tan, R. Zou, J. Zhang, W. Li, L. Zhang, D. Yue, *Nanoscale*, **8**, 4742 (2016).
14. J. Hou, J. Dong, H. Zhu, X. Teng, S. Ai, M. Mang, *Biosens. Bioelectron*., **68**, 20 (2015).
15. T. Han, T. Yan, Y. Li, W. Cao, X. Pang, Q. Huang, Q. Wei, *Carbon*, **91**,144 (2015).
16. S. Y. Lim, W. Shen, Z. Gao, *Chem. Soc. Rev*., **44**, No. 1, 362 (2015).
17. H. Li, Z. Kang, Y. Liu, S. Lee, *J. Mater. Chem*., **22**, No. 46, 24230 (2012).
18. K. Wang, Q. Ji, J. Xu, H. Li, D. Zhang, X. Liu, Y. Wu, H. Fan, *J. Fluoresc*., **28**, 759 (2018).
19. R. Atchudan, T. N. J. I. Edison, D. Chakradhar, S. Perumal, J. Shim, Y. R. Lee, *Sensor. Act. B*, **246**, 497 (2017).
20. S. Sharma, S. K. Mehta, S. K. Kansal, *Sensor. Act. B*, **243**, 1148 (2017).
21. C. Zhang, Y. Cui, L. Song, X. Liu, Z. Hu, *Talanta*, **150**, 54 (2016).
22. J. Wang, F. Qiu, H. Wu, X. Li, T. Zhang, X. Niu, D. Yang, J. Pan, J. Xu, *Spectrochim. Acta A*, **179**, 163 (2017).
23. R. Tabaraki, O. Abdi, S. Yousefipour, *J. Fluoresc*., **27**, 651 (2017).
24. H. Liu, Z. He, L. Jiang, J. Zhu, *ACS Appl. Mater. Int*., **7**, 4913 (2015).
25. H. M. R. Goncalves, A. J. Duarte, J. C. G. E. D. Silva, *Biosens. Bioelectron*., **26**, 1302 (2010).
26. Y. Guo, Z. Wang, H. Shao, X. Jiang, *Carbon*, **52**, 583 (2013).
27. K. Yang, S. Wang, Y. Wang, H. Miao, X. Yang, *Biosens. Bioelectron*., **91**, 566 (2017).
28. E. F. C. Simoes, J. C. G. E. D. Silva, J. M. M. Leitao, *Sensor. Act. B*, **220**, 1043 (2015).
29. M. Luo, Y. Hua, Y. Liang, J. Han, D. Liu, W. Zhao, P. Wang, *Biosens. Bioelectron*., **98**, 195 (2017).
30. W. Yang, J. Ni, F. Luo, W. Weng, Q. Wei, Z. Lin, G. Chen, *Anal. Chem*., **89**, 8384 (2017).
31. P. Devi, G. Kaur, A. Thakur, N. Kaur, A. Grewal, P. Kumar, *Talanta*, **170**, 49 (2017).
32. Z. Li, J. Zhang, Y. Li, S. Zhao, P. Zhang, Y. Zhang, J. Bi, G. Liu, Z. Yue, *Biosens. Bioelectron*., **99**, 251 (2018).
33. J. Hou, H. Li, L. Wang, P. Zhang, T. Zhou, H. Ding, L. Ding, *Talanta*, **146**, 34 (2016).
34. M. K. Gaydhane, P. Choubey, C. S. Sharma, S. Majumdar, *Mater. Today Commun*., **24**, 100953 (2020).
35. A. M. Alak, S. Moy, I. Bekersky, *Ther. Drug Monit*., **18**, 604 (1996).
36. J. L. Italia, D. Singh, M. N. V. R. Kumar, *Anal. Chim. Acta*, **634**, 110 (2009).
37. U. S. Chakrabarty, T. K. Pal, *J. Pharm. Res*., **4**, No. 9, 3194 (2011).
38. X. Xiong, S. Zhai, F. Liu, *Chromatographia*, **70**, 329 (2009).
39. T. Eldem, N. Aricancellat, *J. Pharmaceut. Biomed*., **25**, 53 (2001).
40. Y. Chen, Y. Wu, B. Weng, B. Wang, C. M. Li, *Sensor. Act. B*, **223**, 689 (2016).
41. J. Niu, H. Gao, *J. Lumin*., **149**, 159 (2014).
42. M. Yang, H. Li, J. Liu, W. Kong, S. Zhao, C. Li, H. Huang, Y. Liu, Z. Kang, *J. Mater. Chem. B*, **2**, 7964 (2014).